

# A fully integrated 4.8-6 GHz Power Amplifier with on-chip output balun in 38 GHz-f<sub>T</sub> Si-Bipolar

Student paper

W4  
37

Winfried Bakalski<sup>1,2</sup>, Werner Simbürger<sup>1</sup>, Ronald Thüringer<sup>1,2</sup>,  
Hans-Dieter Wohlmuth<sup>1</sup> and Arpad L. Scholtz<sup>2</sup>

<sup>1</sup> Infineon Technologies AG,  
Otto-Hahn-Ring 6, D-81730 Munich, Germany,  
E-Mail: winfried.bakalski@infineon.com

<sup>2</sup> Institute of Communications and Radio-Frequency Engineering,  
Vienna University of Technology, Gusshausstrasse 25, 1040 Vienna, Austria

**Abstract** A fully integrated radio frequency power amplifier for 4.8-6 GHz has been realized in a 38 GHz-f<sub>T</sub>, 0.25  $\mu$ m-Si-BiCMOS technology. The balanced 2-stage push-pull power amplifier uses two on-chip transformers as input balun and for interstage matching and an LC-type output balun with planar inductors. With this output network no external elements are required. At 1.2 V, 1.5 V, 2 V supply voltages output powers of 17 dBm, 18.9 dBm, 20.7 dBm are achieved at 5.8 GHz. The small-signal gain is 23 dB.

## I. INTRODUCTION

With the boom of wireless LAN chipsets the need of power amplifier solutions for low supply voltage arises. In the past several such power amplifiers for low power voltages have been reported [1], [2], but most of them require an external matching circuitry or do not fit the 5 GHz band. Beside the often found single-ended power amplifiers [3], the only reported differential typed amplifier with an integrated single-ended output solution was presented in [4] for 2.4 GHz in CMOS.

Aim of the work presented here was to realize a fully integrated power amplifier for the 4.8-6 GHz band with no external elements needed. The amplifier circuit is based on two on-chip transformers for the input balun and for interstage matching. The push-pull type circuit configuration, invented in the early days of tubes, has survived into semiconductor era with its benefits. The concept shows a 4:1 load-line impedance benefit for a push-pull combining scheme in an equal power comparison to a single-ended design. This is an advantageous issue at low supply voltages. However, usually an output balun is required. Impedance

mismatch losses at the output of an RF power amplifier due to the decrease of the impedance required at low power supply voltages, conduction losses, charge-storage effects of the transistor and the contrary behaviour of gain and switching speed vs. breakdown voltage limits the maximum available output power and PAE. Therefore, for the first time, an LC-type balun was integrated on-chip including RF-choke and DC-block capacitor to achieve a single-ended 50  $\Omega$  output.

## II. CIRCUIT DESIGN

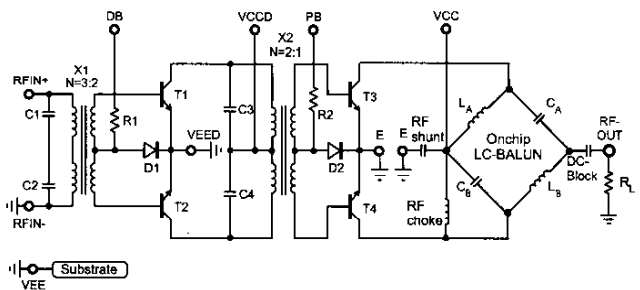


Fig. 1. Circuit diagram of the fully integrated power amplifier.

Fig. 1 shows the circuit diagram of the power amplifier. The circuit consists of a transformer X1 as input balun, a driver stage T1 and T2, a transformer X2 as interstage matching network and the output stage T3 and T4. The bias of the driver stage and the output stage are set by current mirrors D1 and D2, respectively. The effective emitter area of T1, T2 is 40  $\mu\text{m}^2$  and 100  $\mu\text{m}^2$  for T3, T4 each.

X1 is connected as a parallel resonant device with the input capacitors C1 and C2. The transformer acts as balun as well as input matching network. In addition there are several advantages:

- No restrictions to the external DC potential at the input terminals.
- No external DC-block capacitor required.
- The input signal can be applied balanced or unbalanced if one input terminal is grounded.
- Relaxed electrostatic discharge requirements.

The turn ratio of X1 is N=3:2. The size is  $165 \times 165 \mu\text{m}^2$ . The primary winding consists of 3 turns. Metal 1 and Metal 2 are not used to reduce parasitic substrate coupling of the primary winding. Both turns of the secondary winding use also metal 3. The total coupling coefficient is  $k=0.7$  at 5.8 GHz.

Fig. 2 shows the interstage power transformer. X2 is connected as a parallel resonant device with two capacitors C3 and C4. C3 and C4 are connected in antiseries to short the parasitic substrate capacities to the VCCD node. X2 has a turn ratio of N=2:1. The total coupling coefficient is  $k=0.45$  at 5.8 GHz. The size is  $150 \times 150 \mu\text{m}^2$ . The primary winding consists of 2 turns with metal 3 and the secondary of 1 turn also using metal 3. Modeling issues of monolithic transformers are presented in [5], [6], [7], [8].

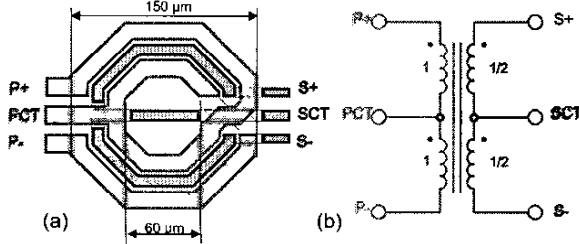


Fig. 2. Interstage power transformer X2: (a) Winding scheme (b) Schematic symbol.

### III. ON-CHIP LC-BALUN DESIGN

During last years several balun concepts have been proposed [9], [10], but most of them result in large structures. The Lattice-type LC-balun [11], [12] is the most compact solution, as it is a solution based on lumped components. Additionally it allows also an impedance transformation and can be realized using transmission lines [13].

The ideal lattice-type balun consists of two inductances  $L_A = L_B$  and two capacitors  $C_A = C_B$  (Fig. 1). An RF choke and a DC-block capacitor are used to feed the supply voltage to the collectors.  $R_1$  is the balanced input impedance of the bridge. Each collector is loaded by  $R_1/2$ .  $R_L$  is the load resistor, usually  $50 \Omega$ .  $L$  and  $C$  can be calculated by

$$L_A = L_B = \frac{Z_1}{\omega_1} \quad (1)$$

$$C_A = C_B = \frac{1}{\omega_1 Z_1} \quad (2)$$

where  $Z_1 = \sqrt{R_1 \cdot R_L}$  is the characteristic impedance of the bridge.  $\omega_1 = 2\pi f_1$  is the frequency of operation.

Unfortunately, the use of bond wires at the RF output leads to a complex valued load impedance. So we use the series circuit of bond-wire and the DC-block capacitor to get a real-valued load. With the knowledge of this real-valued load, the LC-balun can be designed using equations 1 and 2. Interconnections, inductances and parasitic capacitances will shift the calculated values for  $L$  and  $C$ . Additionally, bond wires for the power supply feeding have to be considered as well as the transmission lines at the balun input.

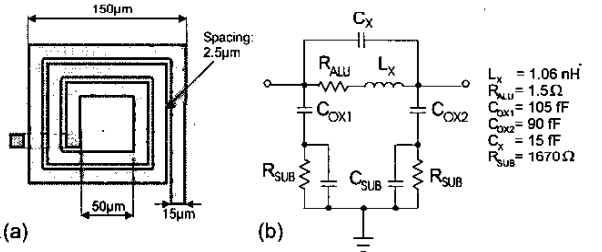


Fig. 3. (a) 1nH Coil (b) Equivalent circuit.

Fig. 3 shows the used coils  $L_A$  and  $L_B$ . The size is  $150 \times 135 \mu\text{m}^2$ . The winding consists of 2.75 turns. metal 1 and metal 2 are not used to reduce parasitic substrate coupling of the winding. The interconnection uses Metal 1 and 2 to have about the same maximum current density applicable. The inductors are modeled with an in-house tool called Coilgen based on Grovers formula [14] and substrate effects presented in [7], [15]. The equivalent circuit for the used coils  $L_A$  and  $L_B$  can be found in Fig. 4. Capacitances and DC-block were realized as metal/isolator/metal capacitors (MIM-CAPs).

### IV. TECHNOLOGY

Fig. 4 shows the die photograph of the fully integrated power amplifier. The die size is  $0.9 \times 1 \text{ mm}^2$ .

The technology used in this work is a  $0.25 \mu\text{m}$  BiCMOS process. It features a bipolar junction transistor with an  $f_T$  of 38 GHz and a three layer metalization with an optional thick upper layer, used for this chip. Further devices

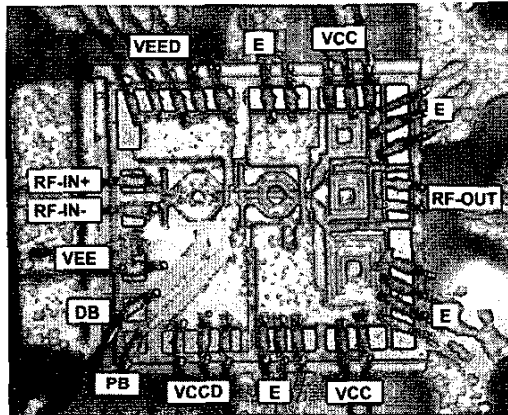


Fig. 4. Die Photograph of the power amplifier  
(size:  $0.9 \times 1 \text{ mm}^2$ ).

are a vertical pnp transistor, poly-Si resistors, MIM capacitors and inductors. The worst-case collector-base breakdown voltage is  $\text{BVCB0} = 8 \text{ V}$  (typical 12 V) and the worst-case collector-emitter breakdown voltage is  $\text{BVCE0} = 2.6 \text{ V}$  (typical 3 V).

## V. EXPERIMENTAL RESULTS

Fig. 5 shows the power amplifier test-board. The substrate parameters are  $\epsilon_r = 3.38$ ,  $\tan \delta = 0.0027$  and the dielectric thickness is 0.51 mm. The metalization layers consist of 18  $\mu\text{m}$  copper with a nickel diffusion barrier and 5  $\mu\text{m}$  gold on top for bonding. The die is attached with a conductive epoxy to the substrate and is bonded directly on the board.

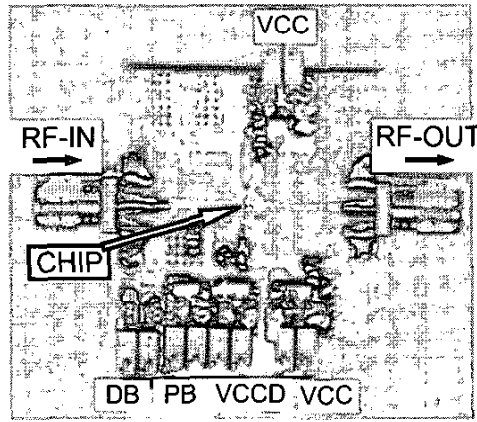


Fig. 5. Photograph of the power amplifier test board  
(size:  $30 \times 30 \text{ mm}^2$ ).

The power amplifier was characterized operating in a pulsed mode with a duty cycle of 12.5% with a pulse width of 600  $\mu\text{s}$  as well as for CW operation (Tab. I).

Fig. 6 shows the measured power transfer characteristic. The maximum output power is 20.7 dBm at 2.0 V supply voltage and 5.8 GHz. The maximum PAE is 14.2%. Fig. 7 shows the characteristic vs. the supply voltage. The linearity for wireless LAN applications was tested using an WLAN-OFDM Error Vector Magnitude measurement setup in CW-mode: The EVM of 3 % is reached for an input power of -8 dBm, next to the compression.

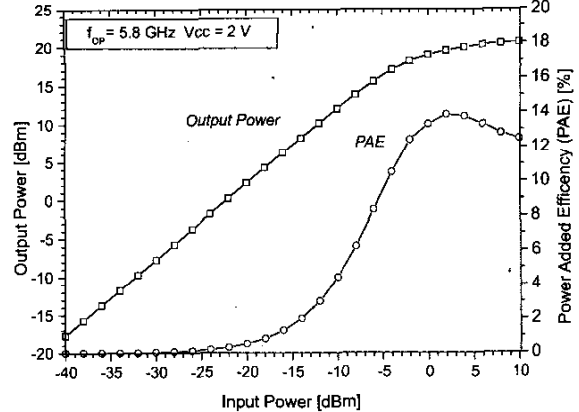


Fig. 6. Measured power transfer characteristic ( $T = 300 \text{ K}$ , 12.5 % duty cycle, 0.600 ms pulse width).

Fig. 8 shows the frequency response. The frequency response shows a high PAE and output power level in a frequency range from  $f = 4.8 \text{ GHz}$  to 6 GHz. Tab. I shows the performance summary.

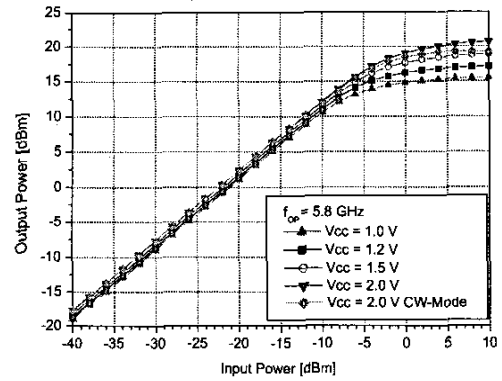


Fig. 7. Measured power transfer characteristic  
vs. supply voltage.

Operating frequency	4.8 GHz – 6 GHz					
Small-signal gain	23 dB					
Supply voltage	1	1.2	1.5	2.0	2.0 CW	V
Maximum output power (5.8 GHz, Pin=10 dBm)	15.5 (36)	17 (50.2)	18.9 (77.6)	20.7 (118)	19.3 (85.2)	dBm mW
Power-added efficiency (5.8 GHz, Pin=0 dBm)	13	14	14.2	14	11	%
Output stage collector current (RF on) + bias	150 + 16	170 + 16	197 + 16	230 + 16	250 + 13.7	mA
Output stage collector current (RF off) + bias	76 + 16	79 + 16	85 + 16	96 + 16	78 + 14.6	mA
Driver stage current (RF on) + bias	50 + 8	52 + 8	55 + 8	55 + 8	78 + 13.6	mA
Driver stage current (RF off) + bias	33 + 8	35 + 8	37 + 8	42 + 8	100 + 12.5	mA

TABLE I. Performance Summary (T=300 K, 12.5 % duty cycle, 0.600 ms pulse width - CW: continuous wave.)

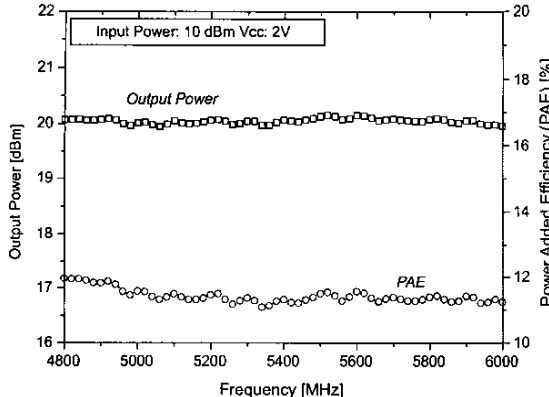


Fig. 8. Measured power amplifier frequency characteristic.

## VI. CONCLUSIONS

We have demonstrated a low voltage power amplifier for 4.8-6 GHz in a 0.25  $\mu$ m-Si-bipolar technology. It is based on a push-pull type circuit with on-chip transformer coupling and on-chip output balun. Thus the amplifier doesn't require any external elements and shows a wide bandwidth of over 1 GHz with a deviation of < 0.3 dB. In CW mode and a supply voltage of 2 V the output power is 19.3 dBm at 5.8 GHz. The maximum output power is 20.7 dBm at 2 V supply voltage. The small signal gain is 23 dB.

## REFERENCES

- [1] Baltus, Peter and van Bezooijen, André, "Design considerations for rf power amplifiers demonstrated through a gsm/edge amplifier module," in *AACD 2001 Workshop*. AACD, April 2001.
- [2] Simbürger, W., Heinz, A., Wohlmuth, H.D., Böck, J., Aufinger, K., and Rest, M., "A Monolithic 2.5V, 1W Silicon Bipolar Power Amplifier with 55% PAE at 1.9 GHz," in *IEEE MTT-S IMS Digest*, Boston, June 2000, IEEE, pp. 853-856.
- [3] Zhang, W., Khoo, E., and Tear, T., "A Low Voltage Fully-Integrated 0.18  $\mu$ m CMOS Power Amplifier for 5GHz WLAN," in *Proceedings of ESSCIRC 2002*, Firenze, Italy, September 2002, IEEE, pp. 215-218.
- [4] Aoki, I., Kee, S.D., Rutledge, D., and Hajimiri, A., "A 2.4 GHz, 2.2 W, 2 V fully integrated CMOS circular geometry active transformer power amplifier," in *IEEE Custom integrated circuits conference*, San Diego, May 2001, IEEE.
- [5] Cheung, D.T.S., Long, J.R., Hadaway, R.A., and Harame, D.L., "Monolithic Transformers for Silicon RF IC Design," in *1998 Bipolar/BiCMOS Circuits and Technology Meeting*, Minneapolis, 27-29 Sept. 1998, IEEE, pp. 105-108.
- [6] J.R. Long, "Monolithic transformers for silicon rf ic design," *IEEE Journal of Solid-State Circuits*, vol. 35, no. 9, pp. 1368-82, 2000.
- [7] Kehrer, D., Simbürger, W., Wohlmuth, H.D., and Scholtz, A.L., "Modeling of Monolithic Lumped Planar Transformers up to 20 GHz," in *IEEE Custom Integrated Circuits Conference CICC 2001*, San Diego, May 2001, pp. 401-404.
- [8] Simbürger, W., Wohlmuth, H.D., Weger, P., and Heinz, A., "A Monolithic Transformer Coupled 5 W Silicon Power Amplifier with 59 % PAE at 0.9 GHz," *IEEE Journal of Solid-State Circuits*, vol. 34, no. 12, pp. 1881-92, December 1999.
- [9] Johnson, Richard C. and Jasik, Henry, *Antenna Engineering Handbook*, McGraw-Hill, New York, second edition, 1984.
- [10] Mongia, R., Bahl, I., and Bhartia, P., *RF and Microwave Coupled-Line Circuits*, Artech House, Norwood, MA 02062, first edition, 1999.
- [11] Peter Vizmuller, *RF Design Guide - Systems, Circuits, and Equations*, Artech House, Norwood, MA 02062, first edition, 1995.
- [12] Steve C. Cripps, *RF Power Amplifiers for Wireless Communications*, Artech House, Norwood, MA 02062, first edition, 1999.
- [13] Bakalski, W., Simbürger, W., Knapp, H., and Scholtz, A.L., "Lumped and Distributed Lattice-type LC-Baluns," in *Proceedings of IEEE International Microwave Symposium*, Seattle, June 2002, IEEE.
- [14] F.W. Grover, *Inductance Calculations*, Dover Publications Inc, New York, 1946.
- [15] Hans-Dieter Wohlmuth, *Monolithische Integration von HF-Oszillatoren in Silizium-Bipolartechnik*, Ph.D. thesis, Technical University of Vienna, June 2000.